HOSTED BY

Available online at www.sciencedirect.com

ScienceDirect

Journal of Computational Design and Engineering 3 (2016) 349–362

www.elsevier.com/locate/jcde

Thermal diffusion and diffusion thermo effects on an unsteady heat and mass transfer magnetohydrodynamic natural convection Couette flow using FEM

R. Srinivasa Raju[a], G. Jithender Reddy[b,*], J. Anand Rao[c], M.M. Rashidi[d,e]

[a]*Department of Mathematics, GITAM University, Hyderabad Campus, Rudraram, Medak 502329, Telangana, India*
[b]*Department of Mathematics, VNR Vignana Jyothi Institute of Engineering and Technology, Hyderabad 500090, Telangana, India*
[c]*Department of Mathematics, Faculty of science, Osmania University, Hyderabad 500007, Telangana, India*
[d]*Shanghai Key Lab of Vehicle Aerodynamics and Vehicle Thermal Management Systems, Tongji University, 4800 Cao An Rd., Jiading, Shanghai 201804, China*
[e]*ENN-Tongji Clean Energy Institute of Advanced Studies, Shanghai, China*

Received 27 January 2016; received in revised form 17 June 2016; accepted 26 June 2016
Available online 1 July 2016

Abstract

The numerical solutions of unsteady hydromagnetic natural convection Couette flow of a viscous, incompressible and electrically conducting fluid between the two vertical parallel plates in the presence of thermal radiation, thermal diffusion and diffusion thermo are obtained here. The fundamental dimensionless governing coupled linear partial differential equations for impulsive movement and uniformly accelerated movement of the plate were solved by an efficient Finite Element Method. Computations were performed for a wide range of the governing flow parameters, viz., Thermal diffusion (Soret) and Diffusion thermo (Dufour) parameters, Magnetic field parameter, Prandtl number, Thermal radiation and Schmidt number. The effects of these flow parameters on the velocity (u), temperature (θ) and Concentration (ϕ) are shown graphically. Also the effects of these pertinent parameters on the skin-friction, the rate of heat and mass transfer are obtained and discussed numerically through tabular forms. These are in good agreement with earlier reported studies. Analysis indicates that the fluid velocity is an increasing function of Grashof numbers for heat and mass transfer, Soret and Dufour numbers whereas the Magnetic parameter, Thermal radiation parameter, Prandtl number and Schmidt number lead to reduction of the velocity profiles. Also, it is noticed that the rate of heat transfer coefficient and temperature profiles increase with decrease in the thermal radiation parameter and Prandtl number, whereas the reverse effect is observed with increase of Dufour number. Further, the concentration profiles increase with increase in the Soret number whereas reverse effect is seen by increasing the values of the Schmidt number.

Keywords: Heat and Mass transfer; Natural convection; MHD; Couette flow; Finite Element Method

1. Introduction

The Couette flow in fluid dynamics refers to the laminar flow of a viscous fluid in the space between the two parallel plates, one of which moves relative to the other. This flow is driven by virtue of viscous drag force acting on fluid and the applied pressure gradient is parallel to the plates. Such flow was named in honor of Maurice Marie Alfred Couette, a professor of Physics at the French University of Angers in the late 19th century. Shear-driven fluid motion is explained in undergraduate physics and engineering courses using Couette flow. Couette motion is applied application viz. magneto hydrodynamics power generators and pumps, petroleum industry, polymer technology, purification of crude oil and fluid droplets sprays. This type of flow was analyzed by Singh et al. [1], Gorla et al. [2] and Kearsley et al. [3]; Umavathi et al. [4] studied the generalized plain heat transfer of Couette flow in a composite channel. The system of non-linear differential equations of a newtonian magnetic lubricant squeeze film flow with magnetic induction effects were solved

*Corresponding author at: Department of Mathematics, VNR Vignana Jyothi Institute of Engineering and Technology, Bachupally, R.R (dist), Hyderabad, 500090, Telangana, India.
E-mail address: jithendergurejala@gmail.com (G. Jithender Reddy).
Peer review under responsibility of Society of CAD/CAM Engineers.

http://dx.doi.org/10.1016/j.jcde.2016.06.003

Nomenclature

List of Variables

h	Distance between two parallel plates (m)
H_o	Magnetic field component along $y'-$ axis (Am^{-1})
C_p	Specific heat at constant pressure $(\mathrm{J\,Kg}^{-1}\,\mathrm{K})$
C_s	Concentration susceptibility $(\mathrm{m\,mole}^{-1})$
Gr	Grashof number for heat transfer
Gc	Grashof number for mass transfer
g	Acceleration of gravity $(\mathrm{m\,s}^{-2})$
M	Hartmann number
Pr	Prandtl number
Sc	Schmidt number
R	Thermal radiation parameter
F	Accelerating parameter
D	Chemical molecular diffusivity $(\mathrm{m}^2\,\mathrm{s}^{-1})$
T'	Temperature of fluid (K)
T'_w	Temperature of the fluid near to moving plate (K)
T'_h	Temperature of the fluid near to the stationary plate (K)
C'	Concentration of fluid $(\mathrm{mol\,m}^{-3})$
C'_w	Concentration of the fluid near to moving plate $(\mathrm{mol\,m}^{-3})$
C'_h	Concentration of the fluid near to the stationary plate $(\mathrm{mol\,m}^{-3})$
t'	Time in x', y' coordinate system (s)
t	Time in dimensionless co-ordinates (s)
u'	Velocity component in $x'-$ direction $(\mathrm{m\,s}^{-1})$
u	Dimensionless velocity component in $x'-$ direction $(\mathrm{m\,s}^{-1})$
Nu_o	Nusselt number at the moving hot plate
Nu_1	Nusselt number at the stationary plate
Sh	Sherwood number
Sr	Soret number (Thermal Diffusion)
Dr	Dufour number (Diffusion Thermo)
q_r	Radiative heat flux
$\overline{K}$	Chemical reaction of first order with rate constant
x', y'	Co-ordinate system (m)
x, y	Dimensionless coordinates (m)
U_o	Reference velocity $(\mathrm{m\,s}^{-1})$
D_m	Mass diffusivity $(\mathrm{m}^2\,\mathrm{s}^{-1})$
T_m	Mean fluid temperature (K)
k_T	Thermal diffusion ratio
k^*	Mean absorption coefficient

Greek symbols

β	Coefficient of volume expansion for heat transfer (K^{-1})
β^*	Coefficient of volume expansion for mass transfer $(\mathrm{m}^3\,\mathrm{kg}^{-1})$
κ	Thermal conductivity of the fluid $(\mathrm{W\,m}^{-1}\,\mathrm{K}^{-1})$
σ	Electrical conductivity of the fluid $(\mathrm{S\,m}^{-1})$
ν	Kinematic viscosity $(\mathrm{m}^2\,\mathrm{s}^{-1})$
θ	Non-dimensional temperature (K)
ϕ	Concentration of the fluid $(\mathrm{mol\,m}^{-3})$
ρ	Density of the fluid $(\mathrm{kg\,m}^{-3})$
α	Angle (degrees)
τ	Skin-friction (pascal)
μ	Viscosity $(\mathrm{m}^2\,\mathrm{s}^{-1})$
$\overline{\sigma}$	Stefan–Boltzmann constant

Superscript

$'$	Dimensionless properties

Subscripts

h	Free stream condition
p	Plate
w	Wall conditions

by Rashidi et al. [5] using the combination of the differential transform and Padé approximation methods. Freidoonimehr et al. [6] investigated the transient magnetohydrodynamic free laminar convective flow of nano-fluid past a vertical porous and stretched surface under acceleration by considering four different types of water based nano-fluid namely, copper (Cu), copper oxide (CuO), aluminum oxide (Al_2O_3), and titanium dioxide (TiO_2) using a fourth order Runge–Kutta method based shooting technique. Abolbashari et al. [7] found analytical results of the fluid flow, heat and mass transfer and entropy generation for the steady laminar non-Newtonian nano-fluid flow induced by a stretching sheet in the presence of velocity slip and convective surface boundary conditions using Optimal Homotopy Analysis method. Rashidi et al. [8] performed the second law of thermodynamics analysis of a rotating porous disk in the presence of a magnetic field with temperature-dependent thermo-physical properties numerically using the fourth-order Runge–Kutta method. Gireesha et al. [9] studied the heat transfer of Couette flow with the presence of dusty fluid by the perturbation method. Rajput et al. [10] analyzed the exact solution of free convection in unsteady MHD Couette flow of a viscous incompressible, electrically conducting fluid between the two vertical parallel plates with the presence of thermal radiation, in the absence of thermal diffusion and diffusion thermo. Recently Das et al. [11,12] studied the analytical solutions of hydromagnetic Couette flow problems with the effect of some physical parameters other than Soret and Dufour. Recently Victor et al. [13] studied the finite element analysis of unsteady MHD radiative natural convection Couette flow between two permeable plates with viscous and joule dissipation in the absence of Soret and Dufour. Seth et al. [14] found the analytic solutions of

unsteady MHD convective Couette flow of a viscous, incompressible, electrically conducting, and temperature dependent heat absorbing fluid within a rotating vertical channel embedded in a fluid saturated porous medium taking Hall current using Laplace transform technique.

Seth et al. [15] studied unsteady hydromagnetic natural convection flow of a viscous, incompressible, electrically conducting and temperature dependent heat absorbing fluid confined within a parallel plate rotating vertical channel in porous medium with the help of Laplace transform technique. The heat transfer affected due to concentration gradient is called Diffusion-thermo or Dufour effect. On the other hand mass transfer affected due to temperature gradient is called Thermal-diffusion or Soret effect. Alam et al. [16] investigated the Dufour and Soret effects on mixed convection flow past a vertical porous flat plate in the presence of variable suction. El-Arabawy et al. [17], Rashidi et al. [18–20] and Srinivasa Raju et al. [21] studied unsteady MHD natural convection flow with varying physical parameters. Chamkha et al. [22] analyzed the combining influence of Soret and Dufour on unsteady heat and mass transfer by MHD mixed convection chemically reacting flow over on a stretched vertical surface. El-Kabeir et al. [23] studied the heat and mass transfer by mixed convection from a vertical slender cylinder with chemical reaction and Soret and Dufour effects. Al-Juma et al. [24] studied Soret and Dufour Effects on heat and mass transfer by free convective flow of a micropolar fluid about a sphere embedded in porous media. Jagdish [25] studied the thermal-diffusion impact on MHD three dimensional natural convective Couette flow by perturbation technique with the presence of chemical reaction and the absence of Diffusion thermo.

Electrically conducting viscous fluid flow between two parallel plates in the presence of a transversely applied magnetic field has several applications in many devices such as magnetohydrodynamic (MHD) power generators, MHD pumps, accelerators, aerodynamics, heating, electrostatic precipitation, polymer technology, petroleum industry, purification of molten metals from non-metallic inclusions and fluid droplets-sprays. The influence of thermal radiation on MHD nanofluid flow between two rotating horizontal plates in the presence of Brownian motion and thermophoresis effects have been studied by Sheikholeslami et al. [26] using the fourth-order Runge–Kutta method. The influence of an external magnetic field on ferro-fluid flow and heat transfer in a semi annulus enclosure with sinusoidal hot wall was investigated by Sheikholeslami and Ganji [27] via Control Volume based Finite Element Method. Sheikholeslami et al. [28] studied the force convection heat transfer in a lid driven semi annulus enclosure in the presence of non-uniform magnetic field and the enclosure is filled with Fe_3O_4-water nanofluid using the Control volume based finite element method. The effect of magnetic field dependent viscosity on free convection heat transfer of nanofluid in an enclosure was investigated by Sheikholeslami et al. [29] with the help of control volume based finite element method. The effect of thermal radiation on Al_2O_3-water nanofluid flow and heat transfer in an enclosure with a constant flux heating element was studied by Sheikholeslami et al. [30] via control volume based finite element method. Sheikholeslami et al. [31] applied control volume based finite element method to solve the governing equations of Ferrohydrodynamic and Magnetohydrodynamic effects by filling the enclosure with ferrofluid by assuming the magnetization of the fluid was varying linearly with temperature and magnetic field intensity. Control volume-based finite element method was applied by Sheikholeslami and Rashidi [32] to Fe_3O_4 -water nanofluid mixed convection heat transfer in a lid-driven semi annulus in the presence of a non-uniform magnetic field. Sheikholeslami et al. [33] studied ferro-fluid flow and heat transfer in a semi annulus enclosure by considering thermal radiation and constant heat flux boundary condition with the help of control volume based finite element method. The behavior of hydrothermal of nano-fluid between two parallel plates was studied by Sheikholeslami [34] using KKL correlation. The characteristics of heat transfer and nanofluid flow between two horizontal parallel plates in a rotating system were investigated by Sheikholeslami et al. [35] via Runge–Kutta method of fourth order. Sheikholeslami et al. [36] found computational results of nanofluid flow and heat transfer in a square enclosure containing a rectangular heated body in the presence of four different types of metal and metal-oxide nanoparticles: alumina (Al_2O_3), copper (Cu), silver (Ag) and titania (TiO_2) using the Lattice Boltzmann method. The effect of non-uniform magnetic field on nanofluid forced convection heat transfer in a lid driven semi-annulus was studied by Sheikholeslami et al. [37] in the presence of Brownian motion and thermophoresis effects via Control volume based finite element method. Sheikholeslami and Ellahi [38] studied three dimensional magnetohydrodynamics nanofluid hydrothermal treatment in a cubic cavity heated from below using the Lattice Boltzmann method. Sheikholeslami and Rashidi [39] studied the combined effects of ferrohydrodynamic and magnetohydrodynamic on ferrofluid flow and heat transfer using the Control volume based finite element method. Sheikholeslami and Abelman [40] studied the effects of magnetic field on nanofluid flow, heat, and mass transfer between two horizontal coaxial cylinders in the presence of viscous dissipation using the fourth-order Runge–Kutta method. The Control Volume based Finite Element Method was applied by Sheikholeslami [41] for solving the governing equations of Ferrofluid flow and heat transfer in the presence of an external variable magnetic field.

A Finite Element Method (abbreviated as FEM) is a numerical technique to obtain an approximate solution to a class of problems governed by elliptic partial differential equations. Such problems are called as boundary value problems as they consist of a partial differential equation and the boundary conditions. It has been applied to a number of physical problems, where the governing differential equations are available. The method essentially consists of assuming the piecewise continuous function for the solution and obtaining the parameters of the functions in a manner that reduces the error in the solution. Sivaiah and Raju [42] studied the effect of Hall current on heat and mass transfer viscous dissipative fluid flow with heat source using the finite element method.

Recently Siva Reddy et al. [43] studied influence of thermal diffusion on unsteady MHD natural convective flow past a semi-infinite vertical plate in the presence of viscous dissipation by the Finite Element Method. Anand Rao et al. [44] considered the effects of chemical reaction with heat absorption on an unsteady MHD free convective fluid flow past a semi-infinite perpendicular plate embedded in a porous medium. Anand Rao et al. [45] demonstrated the combined effects of heat and mass transfer on unsteady MHD flow past a vertical oscillatory plate suction velocity using the finite element method. Anand Rao et al. [46] studied transient flow past an impulsively started infinite flat porous plate in a rotating fluid in the presence of magnetic field with Hall current using the finite element technique. The combined effects of heat and mass transfer on unsteady MHD natural convective flow past an infinite vertical plate enclosed by porous medium in the presence of thermal radiation and Hall Current was investigated by Ramana Murthy et al. [47]. Rao et al. [48] found the numerical results of the non-linear partial differential equations of free convective magnetohydrodynamic flow past semi-infinite moving vertical plate with the effects of thermal radiation and viscous dissipation using finite element technique. Reddy Sheri and Srinivasa Raju [49] studied the effect of viscous dissipation on transient free convection flow past an infinite vertical plate through porous medium in the presence of magnetic field using the finite element technique. Srinivasa Raju [50] studied the combined effects of thermal-diffusion and diffusion-thermo on unsteady free convection fluid flow past an infinite vertical porous plate in the presence of magnetic field and chemical reaction using the finite element technique. Srinivasa Raju et al. [51] studied the application of finite element method to unsteady MHD free convection flow past a vertically inclined porous plate including thermal diffusion and diffusion thermo effects. Srinivasa Raju et al. [52] found both analytical and numerical solutions of unsteady magnetohydrodynamic free convective flow past an exponentially moving vertical plate with heat absorption and chemical reaction.

Therefore the objective of the present paper is to study the thermal diffusion and diffusion thermo effects on an unsteady two-dimensional heat and mass transfer radiative MHD natural convective Couette flow of a viscous, incompressible, electrically conducting fluid between the two vertical parallel plates with suction, embedded in a porous medium, under the influence of a uniform transverse magnetic field with suitable boundary conditions in two cases, impulsive movement and uniformly accelerated movement of the plate . The problem is described by a system of coupled linear partial differential equations, whose exact solution is difficult to obtain, whenever it is possible. Thus, the Finite Element Method is adopted to obtain the solution, which is more economical and flexible from computational point of view. The behaviors of velocity, temperature, concentration, Skin-friction coefficient, Nusselt number and Sherwood numbers has been discussed in detail for variation of thermo physical parameters. The uniqueness (novelty) of this research paper is to study the grid independence of Finite Element Method on unsteady magnetohydrodynamic natural convection flow of incompressible, viscous fluid between two parallel plates surrounded by porous medium. In this research world, no authors studied the study of grid independence of finite element method on Couette flow problems (Fig. 1).

2. Mathematical formulation of the problem

Consider the two-dimensional unsteady natural convective Couette flow of a viscous, electrically conducting fluid past vertical a porous plate with suction, under the influence of a uniform transverse magnetic field, thermal radiation, heat and mass transfer. The following assumptions are listed below:

1. The x' −axis and y' −axis are taken along the plate in the vertical upward and normal direction to the plate respectively.
2. Let the plates be separated by a distance h. Initially, at time $t' \leq 0$, the fluid and the plates of the channel are assumed to be at rest and at same temperature T'_h and concentration C'_h. When time $t' > 0$, the plate (at $y' = 0$) starts moving with time dependent velocity $U_o t'^n$ (U_o being a constant and n being a non-negative integer) in its own plane and at the same time the plate temperature and concentration is raised to T'_w and C'_w respectively while the plate (at $y' = h$) is kept fixed. At the same time $t' > 0$, the wall at $y' = h$ is stationary and maintained at a constant temperature T'_h and constant concentration C'_h.

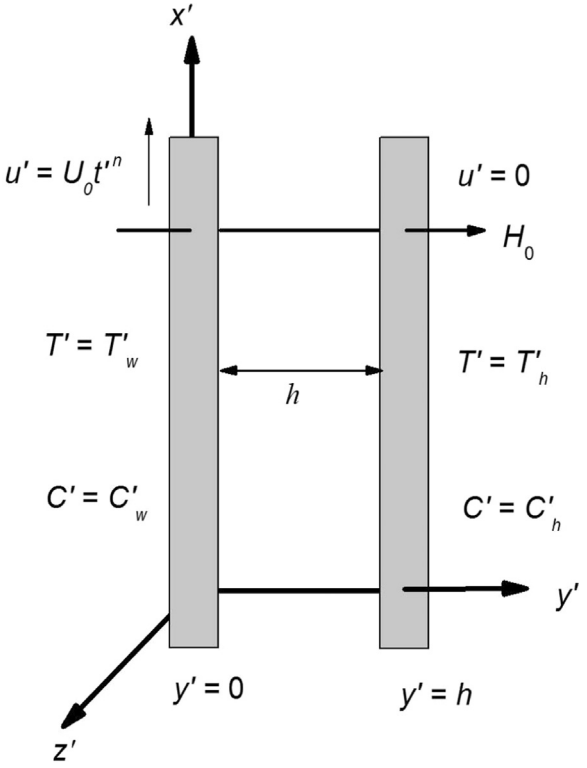

Fig. 1. Physical model in the problem.

3. Assumed transverse magnetic field of the uniform strength H_o is to be applied normal to the plate.
4. The hall effect, viscous dissipation and induced magnetic field are assumed to be negligible because of the magnetic Reynolds number of the flow is considered to be very small.
5. It is assumed that voltage is not applied which implies the absence of an electric field.
6. The homogeneous chemical reaction is of first order with rate constant $\overline{K}$ between the diffusing species and the fluid is neglected.
7. The fluid has constant thermal conductivity and kinematic viscosity, the Boussinesq approximation has been taken for the flow.

From the above assumptions, the unsteady flow is governed by the following partial differential equations.

Momentum equation:

$$\frac{\partial u'}{\partial t'} = \nu \frac{\partial^2 u'}{\partial y'^2} + g\beta\left(T' - T'_h\right) + g\beta^*\left(C' - C'_h\right) - \frac{\sigma \mu_e^2 H_o^2}{\rho}\left(u' - U_o t'^n\right) \tag{1}$$

Energy equation:

$$\frac{\partial T'}{\partial t'} = \frac{\kappa}{\rho C_p}\frac{\partial^2 T'}{\partial y'^2} + \frac{D_m k_T}{C_s C_p}\frac{\partial^2 C'}{\partial y'^2} - \frac{1}{\rho C_p}\frac{\partial q_r}{\partial y'} \tag{2}$$

Species diffusion equation:

$$\frac{\partial C'}{\partial t'} = D\frac{\partial^2 C'}{\partial y'^2} + \frac{D_m k_T}{T_m}\frac{\partial^2 T'}{\partial y'^2} \tag{3}$$

The corresponding initial and boundary conditions are

$$\left.\begin{aligned} &t' \le 0 : u' = 0, \quad T' = T'_h, \quad C' = C'_h \quad for \quad 0 \le y' \le h \\ &t' > 0 : \begin{cases} u' = U_o t'^n, \quad T' = T'_w, \quad C' = C'_w \quad at \quad y' = 0 \\ u' = 0, \quad T' = T'_h, \quad C' = C'_h \quad at \quad y' = h \end{cases} \end{aligned}\right\} \tag{4}$$

The radiative heat flux is simplified by making use of the Rosseland approximation Rajput and Sahu [10] as

$$q_r = -\frac{4\overline{\sigma}}{3k^*}\frac{\partial T'^4}{\partial y'} \tag{5}$$

Following Rajput and Sahu [10], we assume that the differences in temperature within the flow are sufficiently small such that q_r may be expressed as a linear function of T'. Hence on expanding T'^4 in a Taylor Series about T'_h up to first order approximation, we get

$$T'^4 \cong T'^4_h + 4\left(T' - T'_h\right)T'^3_h = 4T'T'^3_h - 3T'^4_h \tag{6}$$

Using Eqs. (5) and (6) in the last term of Eq. (2), we obtain:

$$\frac{\partial q_r}{\partial y'} = -\frac{16\overline{\sigma}T'^3_h}{3k^*}\frac{\partial^2 T'}{\partial y'^2} \tag{7}$$

Introducing (7) in the Eq. (2), the energy equation becomes:

$$\frac{\partial T'}{\partial t'} = \frac{\kappa}{\rho C_p}\frac{\partial^2 T'}{\partial y'^2} + \frac{16\overline{\sigma}T'^3_h}{3k^*\rho C_p}\frac{\partial^2 T'}{\partial y'^2} + \frac{D_m k_T}{C_s C_p}\frac{\partial^2 C'}{\partial y'^2} \tag{8}$$

Introducing the following non-dimensional quantities in Eqs. (1), (3) and (8)

$$\left.\begin{aligned} &u = \frac{u'}{h},\ y = \frac{y'}{h},\ t = \frac{t'\nu}{h^2},\ \theta = \frac{T' - T'_h}{T'_w - T'_h},\ \phi = \frac{C' - C'_h}{C'_w - C'_h}, \\ &Gr = \frac{g\beta h(T'_w - T'_h)}{\nu},\ Gc = \frac{g\beta^* h(C'_w - C'_h)}{\nu}, \\ &F = \frac{U_o h^{2n-1}}{\nu^n},\ M^2 = \frac{\sigma\mu_e^2 H_o^2 h^2}{\rho\nu},\ R = \frac{3\kappa\, k^*}{4\overline{\sigma}T'^3_h}, \\ &\Pr = \frac{\rho\nu C_p}{\kappa},\ Sc = \frac{\nu}{D},\ Dr = \frac{D_m k_T h^2(C'_w - C'_h)}{\nu C_s C_p(T'_w - T'_h)}, \\ &Sr = \frac{D_m k_T(T'_w - T'_h)}{\nu T_m(C'_w - C'_h)},\ \mathrm{Re}_x^{-1} = \frac{U_o x'}{\nu} \end{aligned}\right\} \tag{9}$$

Then the Eqs. (1), (3) and (8) reduce to the following non-dimensional form of equations

$$\frac{\partial u}{\partial t} = \frac{\partial^2 u}{\partial y^2} + Gr\theta + Gc\phi - M^2(u - Ft^n) \tag{10}$$

$$\frac{\partial \theta}{\partial t} = \frac{1}{\Pr}\left(\frac{3R+4}{3R}\right)\frac{\partial^2 \theta}{\partial y^2} + Dr\frac{\partial^2 \phi}{\partial y^2} \tag{11}$$

$$\frac{\partial \phi}{\partial t} = \frac{1}{Sc}\frac{\partial^2 \phi}{\partial y^2} + Sr\frac{\partial^2 \theta}{\partial y^2} \tag{12}$$

Using Eq. (9), the initial and boundary conditions (4) reduce to

$$\left.\begin{aligned} &t \le 0 : u = 0, \quad \theta = 0, \quad \phi = 0 \, for \, 0 \le y \le 1 \\ &t > 0 : \begin{cases} u = Ft^n, \quad \theta = 1, \ \phi = 1 \ at \ y = 0 \\ u = 0, \quad \theta = 0, \quad \phi = 0 \ at \ y = 1 \end{cases} \end{aligned}\right\} \tag{13}$$

Two cases are considered, to find the solutions of Eqs. (10), (11) and (12) subject to the initial and boundary conditions (13):

1. Impulsive movement of the plate at $y' = 0$ (i.e. $n = 0$) and
2. Uniform accelerated movement of the plate at $y' = 0$ (i.e. $n = 1$).

Case (1): Impulsive movement of the plate $y' = 0$:

Taking $n = 0$ in Eq. (10), then the Eq. (10) can be written as

$$\frac{\partial u}{\partial t} = \frac{\partial^2 u}{\partial y^2} + Gr\theta + Gc\phi - M^2(u - F) \tag{14}$$

and the corresponding boundary conditions (13) reduce to

$$\left.\begin{array}{l} t\le 0: \quad u=0,\ \theta=0,\ \phi=0 \ \ for \ \ 0\le y\le 1 \\ t>0: \begin{cases} u=F, & \theta=1, \quad \phi=1 \quad at \quad y=0 \\ u=0, & \theta=0, \quad \phi=0 \quad at \quad y=1 \end{cases} \end{array}\right\} \tag{15}$$

Case (2): Uniform accelerated movement of the plate (at $y'=0$)

Taking $n=1$ in Eq. (10), then the Eq. (10) can be written as

$$\frac{\partial u}{\partial t}=\frac{\partial^2 u}{\partial y^2}+Gr\theta+Gc\phi-M^2(u-Ft) \tag{16}$$

and the initial and boundary conditions (13) reduce to

$$\left.\begin{array}{l} t\le 0: \quad u=0,\ \theta=0,\ \phi=0 \ \ for \ \ 0\le y\le 1 \\ t>0: \begin{cases} u=Ft, & \theta=1, \quad \phi=1 \quad at \quad y=0 \\ u=0, & \theta=0, \quad \phi=0 \quad at \quad y=1 \end{cases} \end{array}\right\} \tag{17}$$

For practical engineering applications and the design of chemical engineering systems, quantities of interest include the following Skin-friction, Nusselt number and Sherwood number which are useful to compute. The skin-friction or the shear stress at the moving plate of the channel in non dimensional form is given by

$$\tau=-\left(\frac{\tau'_w}{\rho u_o v}\right)_{y'=0}=-\left(\frac{\partial u}{\partial y}\right)_{y=0} \tag{18}$$

The rate of heat transfer at the moving hot plate of the channel in non-dimensional form is given by

$$Nu_o=-x'\frac{\left(\frac{\partial T'}{\partial y'}\right)_{y'=0}}{T'_w-T'_\infty}\Rightarrow Nu_o\mathrm{Re}_x^{-1}=-\left(\frac{\partial\theta}{\partial y}\right)_{y=0} \tag{19}$$

Further the rate of heat transfer on the stationary plate is given by

$$Nu_1=-x'\frac{\left(\frac{\partial T'}{\partial y'}\right)_{y'=h}}{T'_w-T'_\infty}\Rightarrow Nu_1\ \mathrm{Re}_x^{-1}=-\left(\frac{\partial\theta}{\partial y}\right)_{y=1} \tag{20}$$

The Sherwood number at the moving plate of the channel in non-dimensional form is given by

$$Sh=-x'\frac{\left(\frac{\partial C'}{\partial y'}\right)_{y'=0}}{C'_w-C'_\infty}\Rightarrow Sh\ \mathrm{Re}_x^{-1}=-\left(\frac{\partial\phi}{\partial y}\right)_{y=0} \tag{21}$$

Where Re_x is the Reynold's number. The mathematical modeling of the problem is now completed. Eqs. (11), (12), (14) and (16) presents a coupled system of linear partial differential equations and these are to be solved with initial and boundary conditions (15) and (17). However, finding the exact solutions are difficult, whenever it is possible. Hence, these equations are solved numerically by the finite element method.

3. Method of solution by Finite Element Method

3.1. Numerical solutions by Finite Element Method

The Finite Element Method (FEM) is an efficient numerical and computational method to solving a variety of engineering and real world problems. It is recognized by so many researchers, developers and users as one of the most powerful numerical analysis tools ever devised to analyze complex problems of engineering. The simplicity of the method, its accuracy and computability all make it a widely used tool in modeling and design process [53]. The primary feature of FEM ([54–56]) is its ability to describe the geometry of the problem being analyzed with great flexibility. This is because of the discretization of domain of the problem is performed using highly flexible elements or uniform or non uniform patches that can be easily depicted as complex shapes. The method essentially consists the piecewise continuous function for the solution and obtaining the parameters of the functions in a systematic manner that reduces the error in the solution. The steps are involved in the finite element analysis as follows.

Step 1: Discretization of the domain: The basic concept of the FEM is to divide the domain or region of the problem into small connected patches, called finite elements. The collection of elements is called the finite element mesh. These finite elements are connected in a non overlapping manner, such that they completely cover the entire space of the problem.

Step 2: Generation of the element equations:

i) A typical element is isolated from the mesh and the variational formulation of the given problem is constructed over the typical element.

ii) Over an element, an approximate solution of the variational problem is supposed, and by substituting this in the system, the element equations are generated.

iii) The element matrix, which is also known as stiffness matrix, is constructed by using the element interpolation functions.

Step 3: Assembly of the element equations: The algebraic equations so obtained are assembled by imposing the inter element continuity conditions. This yields a large number of algebraic equations known as the global finite element model, which governs the whole domain.

Step 4: Imposition of the boundary conditions: The physical boundary conditions defined in (15) and in (17) are imposed on the assembled equations.

Step 5: Solution of assembled equations: The assembled equations so obtained can be solved by any of the numerical techniques, namely, Gauss elimination method, LU decomposition method, and the final matrix equation can be solved by a direct or indirect (iterative) method. For computational purposes, the coordinate y is varied from 0 to $y_{\max}=1$ where $y_{\max}$ represents infinity *i. e.*, external to the momentum, energy and concentration boundary layers. The

whole domain is divided into a set of 100 line segments of equal width 0.1,each element being two-noded.

Variational formulation: The variational formulation associated with Eqs. (10)–(12) over a typical two-noded linear element $(y_e,\ y_{e+1})$ is given by

$$\int_{y_e}^{y_{e+1}} w_1\left[\left(\frac{\partial u}{\partial t}\right)-\left(\frac{\partial^2 u}{\partial y^2}\right)-Gr(\theta)-Gc(\phi)+M^2(u-Ft^n)\right]dy=0 \tag{22}$$

$$\int_{y_e}^{y_{e+1}} w_2\left[\left(\frac{\partial \theta}{\partial t}\right)-\frac{1}{\Pr}\left(\frac{3R+4}{3R}\right)\left(\frac{\partial^2 \theta}{\partial y^2}\right)-Dr\left(\frac{\partial^2 \phi}{\partial y^2}\right)\right]dy=0 \tag{23}$$

$$\int_{y_e}^{y_{e+1}} w_3\left[\left(\frac{\partial \phi}{\partial t}\right)-\frac{1}{Sc}\left(\frac{\partial^2 \phi}{\partial y^2}\right)-Sr\left(\frac{\partial^2 \theta}{\partial y^2}\right)\right]dy=0 \tag{24}$$

where w_1, w_2 and w_3 are arbitrary test functions and may be viewed as the variation in u, θ and ϕ respectively. After reducing the order of integration, we arrive at the following system of equations:

$$\int_{y_e}^{y_{e+1}}\left[(w_1)\left(\frac{\partial u}{\partial t}\right)+\left(\frac{\partial w_1}{\partial y}\right)\left(\frac{\partial u}{\partial y}\right)+(M^2)(w_1)u-(F)(w_1)t^n -(Gr)(w_1)\theta-(Gc)(w_1)\phi\right]dy-\left[(w_1)\left(\frac{\partial u}{\partial y}\right)\right]_{y_e}^{y_{e+1}}=0 \tag{25}$$

$$\int_{y_e}^{y_{e+1}}\left[(w_2)\left(\frac{\partial \theta}{\partial t}\right)+\frac{1}{\Pr}\left(\frac{3R+4}{3R}\right)\left(\frac{\partial w_2}{\partial y}\right)\left(\frac{\partial \theta}{\partial y}\right) +Dr\left(\frac{\partial w_2}{\partial y}\right)\left(\frac{\partial \phi}{\partial y}\right)\right]dy-\left[\left(\frac{w_2}{\Pr}\right)\left(\frac{\partial \theta}{\partial y}\right)+Dr(w_2)\left(\frac{\partial \phi}{\partial y}\right)\right]_{y_e}^{y_{e+1}}=0 \tag{26}$$

$$\int_{y_e}^{y_{e+1}}\left[(w_3)\left(\frac{\partial \phi}{\partial t}\right)+\frac{1}{Sc}\left(\frac{\partial w_3}{\partial y}\right)\left(\frac{\partial \phi}{\partial y}\right)+Sr\left(\frac{\partial w_3}{\partial y}\right)\left(\frac{\partial \theta}{\partial y}\right)\right]dy +\left[\left(\frac{w_3}{Sc}\right)\left(\frac{\partial \phi}{\partial y}\right)+Sr(w_3)\left(\frac{\partial \theta}{\partial y}\right)\right]_{y_e}^{y_{e+1}}=0 \tag{27}$$

Finite element formulation:

The finite element model may be obtained from Eqs. (25)–(27) by substituting finite element approximations of the form:

$$u=\sum_{j=1}^{2}u_j^e\psi_j^e,\quad \theta=\sum_{j=1}^{2}\theta_j^e\psi_j^e,\quad \phi=\sum_{j=1}^{2}\phi_j^e\psi_j^e \tag{28}$$

with $w_1=w_2=w_3=\psi_j^e\ \ (i=1,\ 2)$, where u_j^e ,θ_j^e and $\phi_j^e$are the velocity, temperature and concentration respectively at the j^{th} node of typical e^{th} element $(y_e,\ y_{e+1})$ and ψ_i^e are the shape functions for this element $(y_e,\ y_{e+1})$ and are taken as:

$$\psi_1^e=\frac{y_{e+1}-y}{y_{e+1}-y_e}\quad \text{and}\quad \psi_2^e=\frac{y-y_e}{y_{e+1}-y_e},\quad y_e\le y\le y_{e+1} \tag{29}$$

The finite element model of the equations for e^{th} element thus formed is given by

$$\begin{bmatrix}[K^{11}] & [K^{12}] & [K^{13}]\\ [K^{21}] & [K^{22}] & [K^{23}]\\ [K^{31}] & [K^{32}] & [K^{33}]\end{bmatrix}\begin{bmatrix}\{u^e\}\\ \{\theta^e\}\\ \{\phi^e\}\end{bmatrix} +\begin{bmatrix}[M^{11}] & [M^{12}] & [M^{13}]\\ [M^{21}] & [M^{22}] & [M^{23}]\\ [M^{31}] & [M^{32}] & [M^{33}]\end{bmatrix}\begin{bmatrix}\{u'^e\}\\ \{\theta'^e\}\\ \{\phi'^e\}\end{bmatrix}=\begin{bmatrix}\{b^{1e}\}\\ \{b^{2e}\}\\ \{b^{3e}\}\end{bmatrix} \tag{30}$$

where $\{[K^{mn}],\ [M^{mn}]\}$ and $\{\{u^e\},\{\theta^e\},\{\phi^e\}\ ,\{u'^e\},\ \{\theta'^e\},\ \{\phi'^e\}$ and $\{b^{me}\}\}(m,\ n=1,2,3)$ are the set of matrices of order 2×2 and 2×1 respectively and $'$ (dash) indicates $\frac{d}{dy}$.

These matrices are defined as follows: $K_{ij}^{11}=\int_{y_e}^{y_{e+1}}\left[\left(\frac{\partial \psi_i^e}{\partial y}\right)\left(\frac{\partial \psi_j^e}{\partial y}\right)\right]dy+(M^2)\int_{y_e}^{y_{e+1}}\left(\psi_i^e\right)\left(\psi_j^e\right)dy-Ft^n\int_{y_e}^{y_{e+1}}\left(\psi_i^e\right)dy,$

$K_{ij}^{12}=-Gr\int_{y_e}^{y_{e+1}}\left(\psi_i^e\right)\left(\psi_j^e\right)dy,$

$K_{ij}^{13}=-Gc\int_{y_e}^{y_{e+1}}\left(\psi_i^e\right)\left(\psi_j^e\right)dy,\ M_{ij}^{11}=\int_{y_e}^{y_{e+1}}\left(\psi_i^e\right)\left(\psi_j^e\right)dy,$

$M_{ij}^{12}=M_{ij}^{13}=0,\quad M_{ij}^{21}=M_{ij}^{23}=0,\quad M_{ij}^{31}=M_{ij}^{32}=0,K_{ij}^{21}=0,$

$K_{ij}^{31}=0,b_i^{1e}=\left[\left(\psi_i^e\right)\left(\frac{\partial u}{\partial y}\right)\right]_{y_e}^{y_{e+1}},$

$K_{ij}^{22}=\frac{1}{\Pr}\left(\frac{3R+4}{3R}\right)\int_{y_e}^{y_{e+1}}\left[\left(\frac{\partial \psi_i^e}{\partial y}\right)\left(\frac{\partial \psi_j^e}{\partial y}\right)\right]dy,$

$K_{ij}^{23}=Du\int_{y_e}^{y_{e+1}}\left[\left(\frac{\partial \psi_i^e}{\partial y}\right)\left(\frac{\partial \psi_j^e}{\partial y}\right)\right]dy,$

$K_{ij}^{33}=\frac{1}{Sc}\int_{y_e}^{y_{e+1}}\left[\left(\frac{\partial \psi_i^e}{\partial y}\right)\left(\frac{\partial \psi_j^e}{\partial y}\right)\right]dy,$

$M_{ij}^{22}=\int_{y_e}^{y_{e+1}}\left(\psi_i^e\right)\left(\psi_j^e\right)dy,$-

$b_i^{2e}=\left[\left(\frac{\psi_i^e}{\Pr}\right)\left(\frac{3R+4}{3R}\right)\left(\frac{\partial \theta}{\partial y}\right)+Dr\left(\psi_i^e\right)\left(\frac{\partial \phi}{\partial y}\right)\right]_{y_e}^{y_{e+1}},$

$K_{ij}^{32}=Sr\int_{y_e}^{y_{e+1}}\left[\left(\frac{\partial \psi_i^e}{\partial y}\right)\left(\frac{\partial \psi_j^e}{\partial y}\right)\right]dy,$

$b_i^{3e}=\left[\left(\frac{\psi_i^e}{Sc}\right)\left(\frac{\partial \phi}{\partial y}\right)+Sr\left(\psi_i^e\right)\left(\frac{\partial \theta}{\partial y}\right)\right]_{y_e}^{y_{e+1}}$ and

$M_{ij}^{33}=\int_{y_e}^{y_{e+1}}\left(\psi_i^e\right)\left(\psi_j^e\right)dy.$

In one-dimensional space, linear element, quadratic element, or element of higher order can be taken. The entire flow domain is divided into 10,000 quadratic elements of equal size. Each element is three-noded, and therefore the whole domain contains 20,001 nodes. At each node, three functions are to be evaluated; hence, after assembly of the element equations, we obtain a system of 80,004 equations which are linear. Therefore, an iterative scheme must be utilized in the solution. After imposing the boundary conditions, a system of equations has been obtained which is solved by the Gauss elimination method while maintaining an accuracy of 0.00001. A convergence criterion based on the relative difference between the current and previous iterations is employed. When these differences satisfy the desired accuracy, the solution is

Table 1
The numerical values of u, θ and ϕ for variation of mesh sizes in case-1 (Impulsive movement of the plate at $y' = 0$).

Mesh (Grid) Size = 0.01			Mesh (Grid) Size = 0.001			Mesh (Grid) Size = 0.0001		
u	θ	ϕ	u	θ	ϕ	u	θ	ϕ
1.00000000	1.00000000	1.00000000	1.00000000	1.00000000	1.00000000	1.00000000	1.00000000	1.00000000
1.08651090	0.89902312	0.89773613	1.08803701	0.89906317	0.89810765	1.08953726	0.89910150	0.89844418
1.09550333	0.79818755	0.79592192	1.09836984	0.79826182	0.79660136	1.10118830	0.79833299	0.79721648
1.04589057	0.69756669	0.69469154	1.04977882	0.69766647	0.69559056	1.05360270	0.69776201	0.69640404
0.95372635	0.59720975	0.59410459	0.95822471	0.59732425	0.59512049	0.96265012	0.59743387	0.59603935
0.83178550	0.49713823	0.49414903	0.83643776	0.49725571	0.49517557	0.84101623	0.49736822	0.49610355
0.68943900	0.39734516	0.39475036	0.69379240	0.39745423	0.39568830	0.69807816	0.39755863	0.39653575
0.53281915	0.29779714	0.29578733	0.53646672	0.29788768	0.29655373	0.54005873	0.29797438	0.29724586
0.36523178	0.19843891	0.19711107	0.36784673	0.19850309	0.19764587	0.37042242	0.19856453	0.19812867
0.18776050	0.09919950	0.09856443	0.18912001	0.09923241	0.09883454	0.19045928	0.09926394	0.09907831
0.00000000	0.00000000	0.00000000	0.00000000	0.00000000	0.00000000	0.00000000	0.00000000	0.00000000

Table 2
The numerical values of u, θ and ϕ for variation of mesh sizes in case-2 (Uniform accelerated movement of the plate at $y' = 0$).

Mesh (Grid) Size = 0.01			Mesh (Grid) Size = 0.001			Mesh (Grid) Size = 0.0001		
u	θ	ϕ	u	θ	ϕ	u	θ	ϕ
0.00000000	1.00000000	1.00000000	0.00000000	1.00000000	1.00000000	0.00000000	1.00000000	1.00000000
0.25887764	0.89902312	0.89773613	0.25898206	0.89906317	0.89810765	0.25908482	0.89910150	0.89844418
0.43100041	0.79818755	0.79592192	0.43119749	0.79826182	0.79660136	0.43139136	0.79833299	0.79721648
0.52871627	0.69756669	0.69469154	0.52898526	0.69766647	0.69559056	0.52924997	0.69776201	0.69640404
0.56348127	0.59720975	0.59410459	0.56379491	0.59732425	0.59512049	0.56410354	0.59743387	0.59603935
0.54593152	0.49713823	0.49414903	0.54625863	0.49725571	0.49517557	0.54658055	0.49736822	0.49610355
0.48596683	0.39734516	0.39475036	0.48627543	0.39745423	0.39568830	0.48657909	0.39755863	0.39653575
0.39284736	0.29779714	0.29578733	0.39310774	0.29788768	0.29655373	0.39336395	0.29797438	0.29724586
0.27530533	0.19843891	0.19711107	0.27549303	0.19850309	0.19764587	0.27567768	0.19856453	0.19812867
0.14166926	0.09919950	0.09856443	0.14176714	0.09923241	0.09883454	0.14186347	0.09926394	0.09907831
0.00000000	0.00000000	0.00000000	0.00000000	0.00000000	0.00000000	0.00000000	0.00000000	0.00000000

assumed to have been converged and iterative process is terminated. The Gaussian quadrature is implemented for solving the integrations. The code of the algorithm has been executed twice in MATLAB for case-1(Impulsive movement of the plate at $y' = 0$) and case-2 (Uniform accelerated movement of the plate at $y' = 0$). Excellent convergence was achieved for all the results.

3.2. Study of grid Independence

In general, to study the grid independency/dependency, the mesh size should be varied in order to check the solution at different mesh (grid) sizes and get a range at which there is no variation in the solution. The numerical values of velocity (u), temperature (θ) and concentration (ϕ) for different values of mesh (grid) size are shown in the following Tables 1 and 2 in cases 1 and 2 respectively. From these tables, we observed that, there is no variation in the values of velocity (u), temperature (θ) and concentration (ϕ) for different values of mesh (grid) size. Hence, it is concluded that the results are independent of mesh (grid) size.

Table 3
Values of Skin-friction for various parameters in case of impulsive movement of the plate.

Pr	M^2	R	t	Dr	Sr	τ	Analytical results of Rajput and Sahu [10]
0.71	2.0	1.0	0.02	0	0	3.323170	3.323167
10.0	2.0	1.0	0.02	0	0	2.574285	2.574278
0.71	4.0	1.0	0.02	0	0	3.177202	3.177192
0.71	2.0	2.0	0.02	0	0	3.304121	3.304115
0.71	2.0	1.0	0.04	0	0	1.889310	1.889301
0.71	2.0	1.0	0.02	1	0	4.812012	–
0.71	2.0	1.0	0.02	0	1	4.721561	–

4. Validation of numerical code

In order to check on the correctness of the numerical technique used for the solution of the problem considered in the present study, it was authenticated by performing simulation for numerical solutions for the effect of thermal radiation on unsteady hydromagnetic natural convection Couette flow of a viscous incompressible electrically conducting fluid between

Table 4
Values of Skin-friction for various parameters in case of uniform accelerated movement of the plate.

Pr	M	R	t	F	Dr	Sr	τ	Analytical results of Rajput and Sahu [10]
0.71	2.0	1.0	0.02	0.5	0	0	−0.431103	−0.431103
10.0	2.0	1.0	0.02	0.5	0	0	−0.580015	−0.580015
0.71	4.0	1.0	0.02	0.5	0	0	−0.327830	−0.327830
0.71	2.0	2.0	0.02	0.5	0	0	−0.450175	−0.450175
0.71	2.0	1.0	0.04	0.5	0	0	−0.302497	−0.302497
0.71	2.0	1.0	0.02	0.9	0	0	−0.368107	−0.368107
0.71	2.0	1.0	0.02	0.5	1	0	−0.420381	–
0.71	2.0	1.0	0.02	0.5	0	1	−0.401048	–

Table 5
Results of Nusselt number for various values of physical parameters.

Pr	R	t	Dr	Nu_o	Analytical results of Rajput and Sahu [10]	Nu_1	Analytical results of Rajput and Sahu [10]
0.71	1.0	0.02	0	2.20065	2.20065	0.098109	0.098098
10.0	1.0	0.02	0	8.25878	8.25889	0.002508	0.002487
0.71	2.0	0.02	0	2.60412	2.60384	0.025352	0.025335
0.71	1.0	0.04	0	1.55681	1.55764	0.464661	0.464655
0.71	1.0	0.02	1	2.56812	–	0.106125	–
0.71	1.0	0.02	5	2.75841	–	0.251917	–

two vertical parallel plates which are reported by Rajput and Sahu [10]. Tables 3–5 show the calculated values for Skin-friction, Rate of heat and mass transfer coefficients for the present solution when $Gc = Sr = Dr = 0$, $Sc \to \infty$ and the results are published by Rajput and Sahu [10]. Tables 3–5 show a very good concurrence between the results and this lends credibility to the present numerical code.

5. Results and discussion

To study the effects of different flow parameters like magnetic parameter M, thermal radiation parameter R, Prandtl number Pr, Schmidt number Sc, Accelerating parameter F, Soret number Sr, Dufour number Dr and time t on the flow field, the numerical results of the fluid velocity, temperature, concentration, Skin-friction, Nusselt number and Sherwood number are computed numerically in both the cases viz.

Case (1). Impulsive movement of the plate (at $y' = 0$)
Case (2). Uniform accelerated movement of the plate (at $y' = 0$)

The temperature and the species concentration of the fluid are coupled to the velocity via the Grashof number for heat and mass transfer numbers as seen in Eqs. (14) and (16) in both the cases (1) and (2). The curves in Figs. 2 and 3 illustrate the effects of Grashof numbers for heat and mass transfer on velocity profiles. The relative effect of the thermal buoyancy force to the viscous hydrodynamic force in the boundary layer

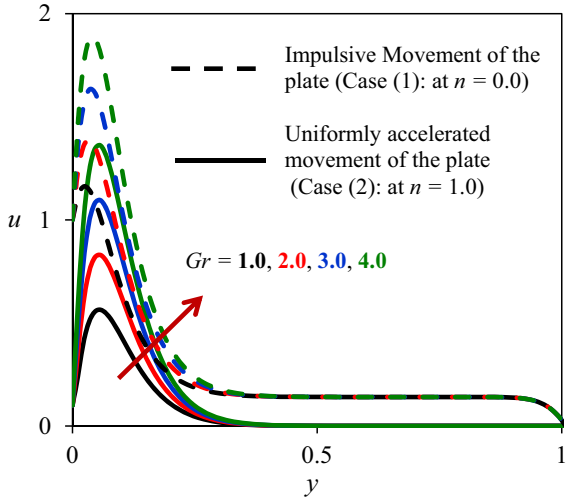

Fig. 2. Velocity profiles for different values of Gr.

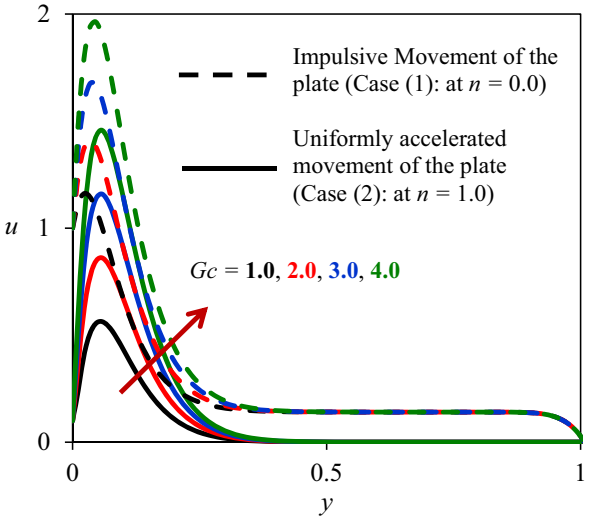

Fig. 3. Velocity profiles for different values of Gc.

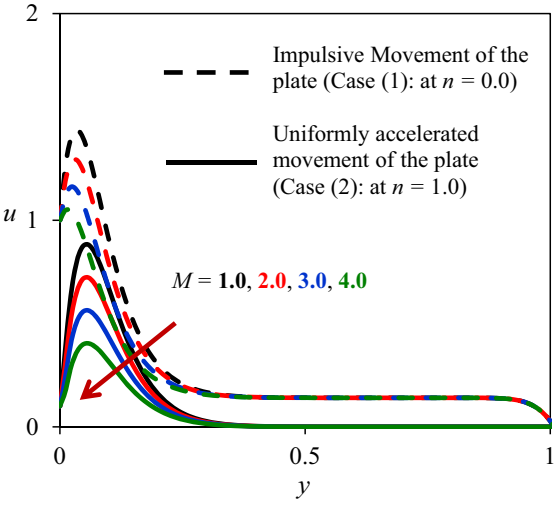

Fig. 4. Velocity profiles for different values of M.

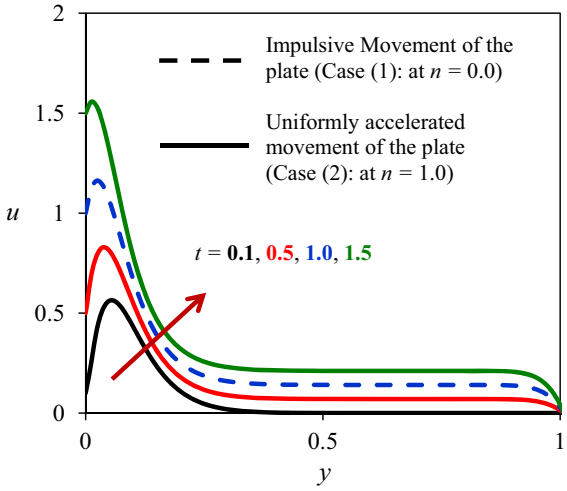

Fig. 5. Velocity profiles for different values of t.

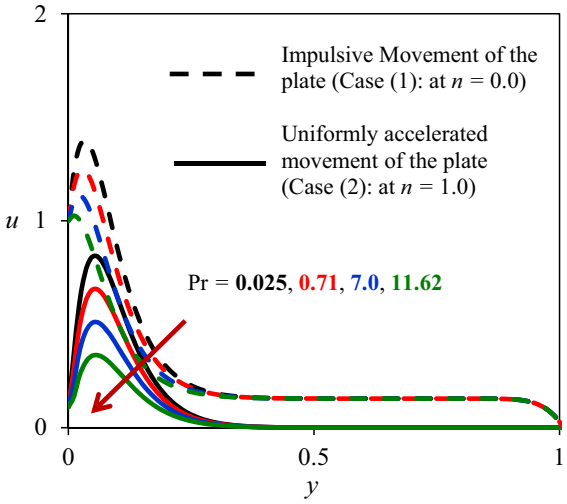

Fig. 6. Velocity profiles for different values of Pr.

is the Grashof number for heat transfer. As expected, it was observed that there was an increase in the velocity due to the enhancement of thermal buoyancy force. Also, as Gr increases, the peak values of the velocity increases rapidly near the porous plate and then decays smoothly to free stream velocity. The ratio of the species buoyancy force to the viscous hydrodynamic force is the Grashof number for mass transfer. As expected, the fluid velocity increases and the peak value is more distinctive due to increase in the species buoyancy force. The velocity distribution attains a distinctive maximum value in the vicinity of the plate and then reduces properly to approach the free stream value. It is noticed that the velocity increases with increasing values of the Grashof number for mass transfer. The influence of Magnetic parameter (Hartmann number) on velocity profiles is as shown in the Fig. 4 by keeping other parameters in rest in both the cases (1) and (2). The presence of a magnetic field in an electrically conducting fluid introduces a force called Lorentz force which acts against the flow if the magnetic field is applied in the normal direction as considered in the present problem. This type of resistive force tends to slow down the flow field. Also, it is observed that the velocity of fluid decreases with increasing magnetic parameter in case of impulsive movement of the plate (i.e. $n = 0$) and in case of uniformly accelerated movement of the plate (i.e. $n = 1$). It is revealed from Fig. 5 that an increase in time leads to rise in the fluid velocity in both the cases (1) and (2). It indicates that there is an enhancement in fluid velocity as time progresses. Figs. 6 and 7 display the effects of Pr (Prandtl number) on the velocity and temperature profiles. The ratio of the viscosity to the thermal diffusivity is the Prandtl number Pr. From these Figs. 6 and 7, it is clear that the velocity and temperature of fluid decreases as the value of Prandtl number increases in both the cases (1) and (2). Physically this is possible because fluids with high Prandtl number have greater viscosity, which make the fluids thick and hence move slowly.

The effect of Schmidt number is very important in both velocity and concentration fields. In both the cases (1) and (2), the effect of the Schmidt number on the velocity and concentration profiles are shown in Figs. 8 and 9, respectively

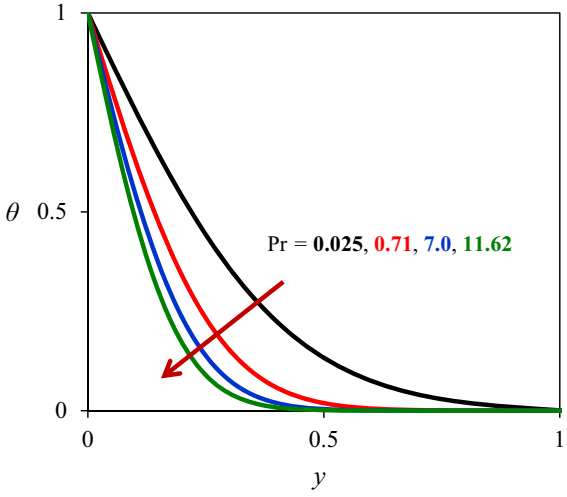

Fig. 7. Temperature profiles for different values of Pr.

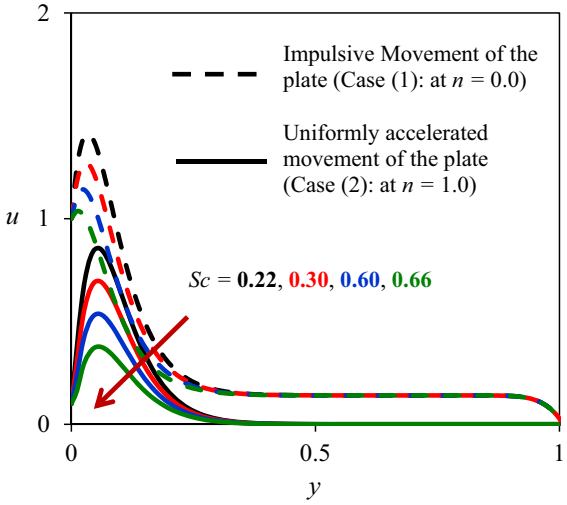

Fig. 8. Velocity profiles for different values of Sc.

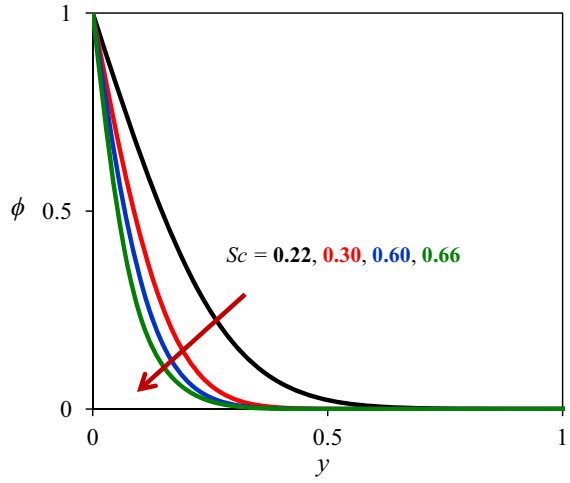

Fig. 9. Concentration profiles for different values of *Sc*.

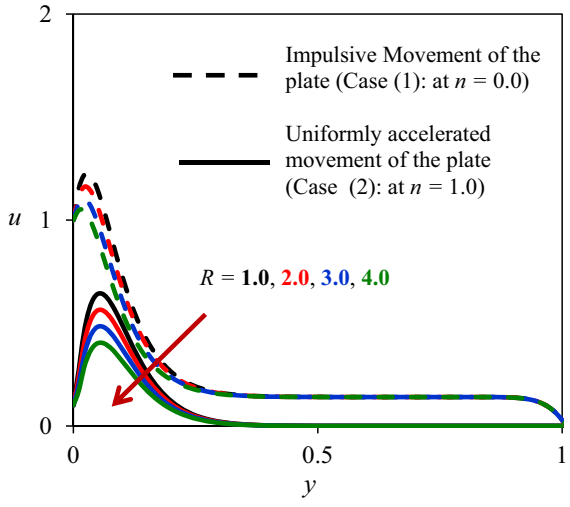

Fig. 10. Velocity profiles for different values of *R*.

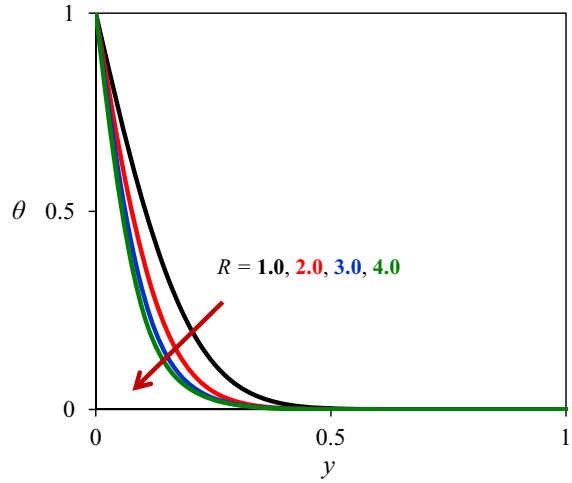

Fig. 11. Temperature profiles for different values of *R*.

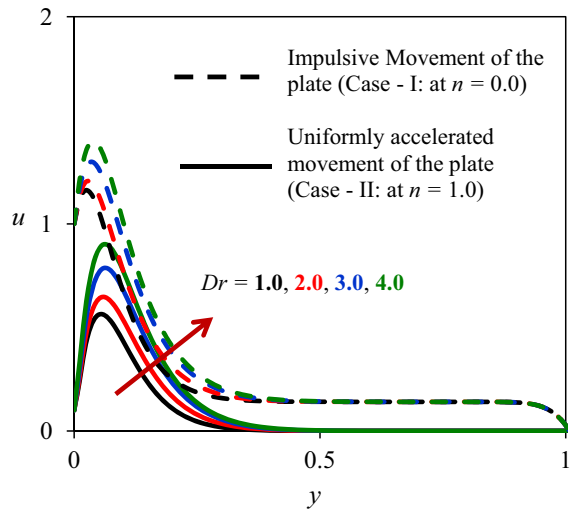

Fig. 12. Velocity profiles for different values of *Dr*.

for various gases like hydrogen (*Sc*=0.22), helium (*Sc*=0.30), water vapor (*Sc*=0.60) and oxygen (*Sc*=0.66). As the Schmidt number increases, the velocity decreases in Fig. 8. This causes the concentration buoyancy effect to decrease yielding a reduction in the fluid velocity. Reductions in the velocity and concentration distributions are accompanied by simultaneous reductions in the velocity and concentration boundary layers. Fig. 9 shows the concentration field due to variation in Schmidt number for the gasses hydrogen, helium, water–vapor and oxygen. It is noticed that the concentration of the fluid decreases as the Schmidt number increases. The concentration falls gradually and progressively for hydrogen in distinction to other gases. Physically, it is true since increase of *Sc* means decrease of molecular diffusivity, which results in decrease of concentration boundary layer. Hence, the concentration of species is smaller for higher values of *Sc*. The effects of the thermal radiation parameter on the velocity and temperature profiles in the boundary layer are illustrated in Figs. 10 and 11 respectively in both the cases (1) and (2). The thermal radiation parameter defines the relative contribution of the conduction heat transfer to thermal radiation transfer. It is obvious that an increase in the thermal radiation parameter results in decreasing velocity and temperature within the boundary layer, as well as a decreased thickness of the velocity and temperature boundary layers. This is because the large *R* -values correspond to an increased dominance of conduction over radiation thereby decreasing buoyancy force (thus, vertical velocity) and thickness of the thermal and momentum boundary layers. In both the cases (1) and (2), the influence of Dufour number (*Dr*) for different values on velocity and temperature profiles are plotted in Figs. 12 and 13 respectively. The Dufour number signifies the contribution of the concentration gradients to the thermal energy flux in the flow. It is found that an increase in the Dufour number causes a rise in the velocity and temperature throughout the boundary layer as the temperature profiles decay smoothly from the plate to the free stream value. However, a distinct velocity overshoot exists near the plate, and thereafter the profile falls to zero at the edge of the boundary layer. Figs. 14 and 15 depict the velocity and concentration profiles for different values of the Soret number

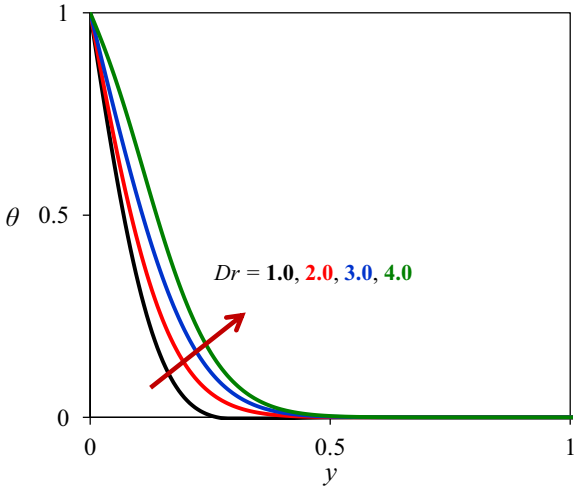

Fig. 13. Temperature profiles for different values of *Dr*.

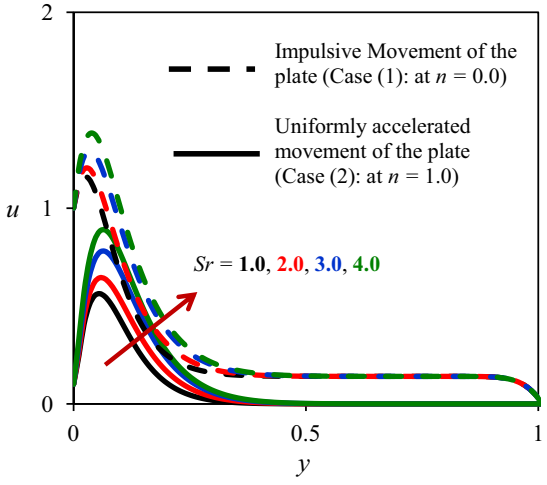

Fig. 14. Velocity profiles for different values of *Sr*.

(*Sr*) in both the cases (1) and (2). The Soret number defines the effect of the temperature gradients inducing significant mass diffusion effects. It is noticed that an increase in the Soret number results in an increase in the velocity and concentration within the boundary layer.

Table 3 shows variation of Skin-friction with the effects of Prandtl number, Magnetic parameter, Thermal radiation parameter, time, Dufour number and Soret number in case of Impulsive movement of the plate. From this table, it is observed that the skin-friction decreases with increasing of magnetic parameter, Prandtl number and radiation parameter and time while decrease with increasing of Dufour and Soret numbers. Table 4 shows the effects of Prandtl number, Magnetic parameter, Thermal radiation parameter, time, Accelerating parameter, Dufour number and Soret number in case of uniformly accelerated movement of the plate. From this table, it is observed that the skin-friction decreases with increasing of Prandtl number and Radiation parameter while increases with increasing of Magnetic parameter, time, Accelerating parameter, Dufour and Soret numbers. Table 5 shows the effect of radiation parameter, Prandtl number, time and Dufour number on the

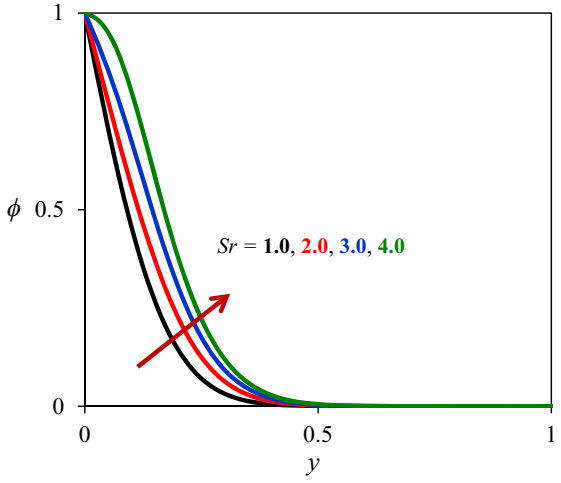

Fig. 15. Concentration profiles for different values of *Sr*.

Table 6
Results of Sherwood Number.

Sc	*Sr*	S_h
0.22	0	1.205984
0.66	0	1.065442
0.22	1	1.424313
0.22	5	2.125932

Nusselt number (the rate of heat transfer) at the moving and stationary plates. We see that the Nusselt number at the moving plate Nu_o increases with increasing values of radiation parameter and Prandtl number while decreases with increasing values of time and Dufour number. The Nusselt number at the stationary plate Nu_1 is decreasing with increasing values of Radiation parameter and Prandtl number while increasing with increasing values of time and Dufour number. Table 6 shows the effect of Schmidt number on the Sherwood number (the rate of mass transfer). From this table, we see that the Sherwood number is decreasing with increasing values of Schmidt number while increases with increasing of Soret number.

6. Conclusion

The present paper studies the effects of radiation, heat and mass transfer on an unsteady two-dimensional natural convective Couette flow of a viscous, incompressible, electrically conducting fluid between two parallel plates with suction, embedded in a porous medium, under the influence of a uniform transverse magnetic field. The problem is described by a system of coupled linear partial differential equations, and is solved by the finite element method. A parametric study is performed to illustrate the influence of thermo physical parameters on the velocity, temperature and concentration profiles. It has been shown that:

1. In both cases the fluid velocity increases with increasing of *Dr*, *Sr* and time *t* while decreases with increasing of *M*, Pr.

2. The fluid temperature increases with increasing of *Dr* and time *t* while decreases with increasing of Pr and *R*.
3. The fluid concentration increases with increasing of *Sr* while decreases with increasing of *Sc*.
4. The skin-friction decreases with increasing of *M*, Pr and *R* and time *t* while decreases with increasing of *Dr* and *Sr* in case of impulsive movement of the plate.
5. The skin-friction decreases with increasing of Pr and *R* while increases with increasing of *M*, time *t, F, Dr* and *Sr* in case of uniform accelerated movement of the plate.
6. The rate of heat transfer Nu_o at the moving plate increases with increasing of *R* and Pr while decreases with increasing values of time *t* and *Dr*.
7. The rate of heat transfer at the stationary plate Nu_1 is decreasing with increasing of *R* and Pr while increases with increasing of time *t* and *Dr*.
8. The rate of mass transfer decreases with increasing of *Sc* while increases with increasing of Soret number *Sr*.
9. In order to ascertain the accuracy of the numerical results, the present results are compared with the previous results of Rajput and Sahu [10] with the absence of *Gc*, *Sc*, *Sr* and *Dr*. They are found to be in an excellent agreement.

Acknowledgment

The authors thank the reviewers for their constructive suggestions and comments, which have improved the quality of the article considerably. Also, the first and second authors are thankful to Dr. K. Tejaswani, GITAM University for her valuable suggestions, continuous support and encouragement in the preparation of this manuscript.

References

[1] Singh AK. Natural convection in unsteady Couette motion. *Def. Sci. J.* 1988;**38**(**1**)35–41.
[2] Gorla RSR, Bartrand TA. Couette flow heat loss model for the rotary combustion engine. *J. Mech. Eng. Sci., Proc. Inst. Mech. Eng.* 1996;**210**:587–96.
[3] Kearsley AJ. A steady state model of Couette flow with viscous heating. *Int. J. Eng. Tech. Res.* 1994;**32**:**1**79–186.
[4] Umavathi JC, Chamkha AJ, Sridhar KSR. Generalized plain Couette flow and heat transfer in a composite channel. *Transp. Porous Media* 2010;**85**:157–69.
[5] Rashidi MM, Freidoonimehr N, Momoniat E, Rostami B. Study of nonlinear MHD tribological squeeze film at generalized magnetic Reynolds numbers using DTM. *PLoS ONE* 2015;**10**(**8**) e0135004 http://dx.doi.org/ 10.1371/journal.pone.0135004.
[6] Freidoonimehr Navid, Rashidi Mohammad Mehdi, Mahmud Shohel. Unsteady MHD free convection flow past a porous stretching vertical surface in a nano-fluid. *Int. J. Therm. Sci.* 2015;**87**:136–45.
[7] Abolbashari Mohammad Hossein, Freidoonimehr Navid, Nazari Foad, Rashidi Mohammad Mehdi. Analytical modeling of entropy generation for Casson nano-fluid flow induced by a stretching surface. *Adv. Powder Technol.* 2015;**26**(**2**)542–52.
[8] Rashidi MM, Mahmud S, Freidoonimehr N, Rostami B. Analysis of entropy generation in an MHD flow over a rotating porous disk with variable physical properties. *Int. J. Exergy* 2015;**16**(4)481–503.
[9] Gireesha BJ, Chamkha AJ, Vishalakshi CS, Bagewadi CS. Three dimensional Couette flow of a dusty fluid with heat transfer. *Appl. Math. Model* 2012;**36**:683–701.
[10] Rajput US, Sahu PK. Natural convection in unsteady hydromagnetic Couette flow through a vertical channel in the presence of thermal radiation. *Int. J. Appl. Math. Mech* 2012;**8**(**3**)35–56.
[11] Das S, Jana RN, Chamkha AJ. Entropy generation in a rotating Couette flow with Suction/Injection. *Commun. Numer. Anal.* 2015;**1**:62–81.
[12] Das S, Jana RN, Chamkha AJ. Entropy generation due to unsteady hydromagnetic Couette flow and heat transfer with asymmetric convective cooling in a rotating system. *J. Math. Model* 2015;**3**:107–28.
[13] Job Victor M, Gunakala Sreedhara Rao. Finite element analysis of unsteady radiative MHD natural convection Couette flow between permeable plates with viscous and joule dissipation. *Int. J. Pure Appl. Math.* 2015;**99**(**2**)123–43.
[14] Seth GS, Sharma Rohit, Kumbhakar B. Effects Of Hall current on unsteady MHD convective Couette flow of heat absorbing fluid due to accelerated movement of one of the plates of the channel in a porous medium. *J. Porous Media* 2016;**19**(**1**)13–30.
[15] Seth GS, Kumbhakar B, Sharma R. Unsteady hydromagnetic natural convection flow of a heat absorbing fluid within a rotating vertical channel in porous medium with Hall effects. *J. Appl. Fluid Mech.* 2015;**8**(**4**)767–79.
[16] Alam MS, Rahman MM. Dufour and Soret effects on mixed convection flow past a vertical porous flat plate with variable suction. *Nonlinear Anal.: Model Control* 2006;**11**(**1**)3–12.
[17] El-Arabawy Hassan AM. Soret and Dufour effects on natural convection flow past a vertical surface in a porous medium with variable Surface temperature. *J. Math. Stat.* 2009;**5**(**3**)190–8.
[18] Rashidi MM, Hayat T, Erfani E, Mohimanian Pour SA, Hendi Awatif A. Simultaneous effects of partial slip and thermal-diffusion and diffusion-thermo on steady MHD convective flow due to a rotating disk. *Commun. Nonlinear Sci. Numer. Simul.* 2011;**16**(11)4303–17.
[19] Rashidi MM, Rastegari MT, Anwar Bég O. Homotopy analysis of Soret and Dufour effects on free convection non-Newtonian flow in a porous medium with thermal radiation flux. *Int. J. Appl. Math. Mech.* 2013;**9**(**2**)39–68.
[20] Rashidi MM, Hayat T, Erfani E, Mohimanian Pour SA, A-Hendi Awatif. Simultaneous effects of partial slip and thermal-diffusion and diffusion-thermo on steady MHD convective flow due to a rotating disk. *Commun. Nonlinear Sci. Numer. Simul.* 2011;**16**:4303–17.
[21] Srinivasa Raju R, Sudhakar K, Rangamma M. The effects of thermal radiation and heat source on an unsteady MHD free convection flow past an infinite vertical plate with thermal diffusion and diffusion thermo. *J. Inst. Eng. (India): Ser. C* 2013;**94**(**2**)175–86.
[22] Chamkha AJ, EL-Kabeir SM. Unsteady heat and mass transfer by MHD mixed convection flow over an impulsively stretched vertical surface with chemical reaction and Soret and Dufour effects. *Chem. Eng. Commun.* 2013;**200**:1220–36.
[23] El-Kabeir SMM, Chamkha AJ. Heat and mass transfer by mixed convection from a vertical slender cylinder with chemical reaction and Soret and Dufour effects. *Heat Transf.-Asian Res.* 2013;**42**:618–29.
[24] Al-Juma N, Chamkha AJ. Soret and Dufour effects on heat and mass transfer by free convective flow of a micropolar fluid about a sphere embedded in porous media. *Int. J. Energy Technol.* 2014;**6**(**8**)1–7.
[25] Prakash Jagdish, Balamurugan Kuppareddy Subramanyam, Varma Sibayala Vijayakumar. Thermo-diffusion and chemical reaction effects on MHD three dimensional free convective Couette flow. *Walailak J. Sci. Tech.* 2015;**12**(**9**)805–30.
[26] Sheikholeslami Mohsen, Ganji Davood Domiri, Javed M Younus, Ellahic R. Effect of thermal radiation on magnetohydrodynamics nanofluid flow and heat transfer by means of two phase model. *J. Magn. Magn. Mater.* 2015;**374**(**15**)36–43.
[27] Sheikholeslami Mohsen, Ganji Davood Domiri. Ferrohydrodynamic and magnetohydrodynamic effects on ferro-fluid flow and convective heat transfer. *Energy* 2014;**75**:400–10.
[28] Sheikholeslami M, Rashidi MM, Ganji DD. Effect of non-uniform magnetic field on forced convection heat transfer of image-water nanofluid. *Comput. Methods Appl. Mech. Eng.* 2015;**294**:299–312.

[29] Sheikholeslami M, Rashidi MM, Hayat T, Ganji DD. Free convection of magnetic nanofluid considering MFD viscosity effect. *J. Mol. Liq.* 2016;**218**:393–9.
[30] Sheikholeslami M, Hayat T, Alsaedi A. MHD free convection of Al2O3-water nanofluid considering thermal radiation: a numerical study. *Int. J. Heat Mass Transf.* 2016;**96**:513–24.
[31] Sheikholeslami Mohsen, Vajravelu Kuppalapalle, Rashidi Mohammad Mehdi. Forced convection heat transfer in a semi annulus under the influence of a variable magnetic field. *Int. J. Heat Mass Transf.* 2016;**92**:339–48.
[32] Sheikholeslami M, Rashidi MM. Ferrofluid heat transfer treatment in the presence of variable magnetic field. *Eur. Phys. J.* 2015;**130**:115, http://dx.doi.org/10.1140/epjp/i2015-15115-4.
[33] Sheikholeslami Mohsen, Ganji Davood Domiri, Rashidi Mohammad Mehdi. Ferro-fluid flow and heat transfer in a semi annulus enclosure in the presence of magnetic source considering thermal radiation. *J. Taiwan Inst. Chem. Eng.* 2015;**47**:6–17.
[34] Kandelousi Mohsen Sheikholeslami. KKL correlation for simulation of nanofluid flow and heat transfer in a permeable channel. *Phys. Lett. A* 2014;**387**(**45**)3331–9.
[35] Sheikholeslami Mohsen, Abelman Shirley, Ganji Davood Domiri. Numerical simulation of MHD nanofluid flow and heat transfer considering viscous dissipation. *Int. J. Heat Mass Transf.* 2014;**79**:212–22.
[36] Sheikholeslami M, Ashorynejad HR, Rana P. Lattice Boltzmann simulation of nanofluid heat transfer enhancement and entropy generation. *J. Mol. Liq.* 2016;**214**:86–95.
[37] Sheikholeslami M, Rashidi MM, Ganji DD. Numerical investigation of magnetic nanofluid forced convective heat transfer in existence of variable magnetic field using two phase model. *J. Mol. Liq.* 2015;**212**:117–26.
[38] Sheikholeslami M, Ellahi R. Three dimensional mesoscopic simulation of magnetic field effect on natural convection of nanofluid. *Int. J. Heat Mass Transf.* 2015;**89**:799–808.
[39] Sheikholeslami Mohsen, Rashidi Mohammad Mehdi. Effect of space dependent magnetic field on free convection of Fe_3O_4-water nanofluid. *J. Taiwan Inst. Chem. Eng.* 2015;**56**:6–15.
[40] Sheikholeslami M, Abelman S. Two-phase simulation of nano-fluid flow and heat transfer in an annulus in the presence of an axial magnetic field. *IEEE Trans. Nanotechnol.* 2015;**14**(**3**)561–9.
[41] Kandelousi Mohsen Sheikholeslami. Effect of spatially variable magnetic field on ferro-fluid flow and heat transfer considering constant heat flux boundary condition. *Eur. Phys. J.* 2014;**129**:248.
[42] Sivaiah S, Srinivasa Raju R. Finite element solution of heat and mass transfer flow with Hall current heat source and viscous dissipation. *Appl. Math. Mech.* 2013;**34**:559–70.
[43] Sheri Siva Reddy, Srinivasa Raju, Soret R. effect on unsteady MHD free convective flow past a semi-infinite vertical plate in the presence viscous dissipation. *Int J Comput Methods Eng Sci Mech* 2015;**16**(**2**)132–41.
[44] Anand Rao J, Sivaiah S, Srinivasa Raju R. Chemical reaction effects on an unsteady MHD free convection fluid flow past a semi-infinite vertical plate embedded in a porous medium with heat absorption. *J. Appl. Fluid Mech.* 2012;**5**:63–70.
[45] Anand Rao J, Srinivasa Raju R, Sivaiah S. Finite element solution of heat and mass transfer in MHD flow of a viscous fluid past a vertical plate under oscillatory suction velocity. *J. Appl. Fluid Mech.* 2012;**5**:1–10.
[46] Anand Rao J, Srinivasa Raju R, Sivaiah S. Finite element solution of MHD transient flow past an impulsively started infinite horizontal porous plate in a rotating fluid with Hall current. *J. Appl. Fluid Mech.* 2012;**5**:105–12.
[47] Ramana Murthy MV, Srinivasa Raju R, Anand Rao J. Heat and mass transfer effects on MHD natural convective flow past an infinite vertical porous plate with thermal radiation and Hall current. *Procedia Eng. J.* 2015;**127**:1330–7.
[48] Rao VS, Babu LA, Raju RS. Finite element analysis of radiation and mass transfer flow past semi-infinite moving vertical plate with viscous dissipation. *J. Appl. Fluid Mech.* 2013;**6**:321–9.
[49] Sheri Siva Reddy, Srinivasa Raju R. Transient MHD free convective flow past an infinite vertical plate embedded in a porous medium with viscous dissipation. *Meccanica* 2016;**51**(**5**)1057–68.
[50] Srinivasa Raju R. Combined influence of thermal diffusion and diffusion thermo on unsteady hydromagnetic free convective fluid flow past an infinite vertical porous plate in presence of chemical reaction. *J. Inst. Eng. (India): Ser. C* 2016, http://dx.doi.org/10.1007/s40032-016-0258-5.
[51] Srinivasa Raju R, Mahesh Reddy B, Rashidi MM, Gorla RSR. Application of finite element method to unsteady MHD free convection flow past a vertically inclined porous plate including thermal diffusion and diffusion thermo effects. *J. Porous Media* 2016. In Press.
[52] Srinivasa Raju R, Jithender Reddy G, Anand Rao J, Rashidi MM, Reddy Gorla Rama Subba. Analytical and numerical study of unsteady MHD free convection flow over an exponentially moving vertical plate with heat absorption. *Int. J. Therm. Sci.* 2016;**107**:303–15.
[53] Charanjiv Gupta, Sanjay Marwaha, Manpreet Singh Manna, Finite element method as an aid to machine design: a computational tool, in: Excerpt from the Proceedings of the COMSOL Conference, Bangalore, 2009.
[54] Bathe KJ. *Finite Element Procedures*. New Jersy: Prentice-Hall; 1996.
[55] Reddy JN. *An Introduction to the Finite Element Method*. New York: McGraw-Hill; 1985.
[56] Zienkiewicz OC. *The Finite Element Method in Engineering Science*, 2nd edn., New York: McGraw-Hill; 1971.